Prospect for tunneling anisotropic magneto-resistance in ferrimagnets: Spin-orbit coupling effects in Mn_3Ge and Mn_3Ga

S. Khmelevskyi, A. B. Shick, and P. Mohn

Citation: Appl. Phys. Lett. **109**, 222402 (2016); doi: 10.1063/1.4970691
View online: http://dx.doi.org/10.1063/1.4970691
View Table of Contents: http://aip.scitation.org/toc/apl/109/22
Published by the American Institute of Physics

Prospect for tunneling anisotropic magneto-resistance in ferrimagnets: Spin-orbit coupling effects in Mn_3Ge and Mn_3Ga

S. Khmelevskyi,[1,a)] A. B. Shick,[2] and P. Mohn[1]
[1]*Center for Computational Materials Science, Vienna University of Technology, Wiedner Hauptstrasse 8-10, 1040 Vienna, Austria*
[2]*Institute of Physics ASCR, Na Slovance 2, 18221 Prague, Czech Republic*

(Received 28 July 2016; accepted 16 November 2016; published online 30 November 2016)

Magnetic anisotropic phenomena in Mn_3Ge and Mn_3Ga ferrimagnets are studied by first-principles density functional theory calculations. We find a large positive magnetic anisotropy energy, associated with the Mn-atoms in the 4d-crystallographic positions. Sizable anisotropy in the density of states is found in the vicinity of the Fermi energy, and suggests the promising possibility for the generation of a sizable tunneling anisotropic magneto-resistance effect (TAMR). The use of the ferrimagnetic materials for TAMR magnetic tunneling junctions is discussed as a prospective alternative for ferromagnetic and antiferromagnetic materials. *Published by AIP Publishing*. [http://dx.doi.org/10.1063/1.4970691]

Development of the magnetic materials for applications in magnetic tunnel junctions (MTJ) used in modern magnetic random access memory (MRAM) devices is a key ingredient for success in the emerging non-volatile memory technologies.[1] The MTJ based devices utilize a large tunneling magneto-resistance effect (TMR) due to the opposite spin-polarization of two active ferromagnetic layers. The size of the resulting TMR ratio, a strong perpendicular magnetic anisotropy (PMA) to ensure the thermal stability, interface matching (growing conditions) and geometrical size effects (demagnetizing fields and magnetic fields straying from the reference magnetic layer) put stringent requirements on the choice of the materials for MTJs.

Recently a class of tetragonal Mn based ferrimagnetic alloys close to the Mn_3X (where X = Ga, Ge) has been studied intensely as candidates to replace the ferromagnetic alloys with large PMA in the TMR devices.[2–7] Thin films of these alloys have a very large PMA and high magnetic ordering temperature[3,5,8,9] and were grown on various substrates. Apart from their large PMA value, the use of the ferrimagnetic layers with a small net magnetization in TMR MTJs can help to reduce the stray field of the reference magnetic layer.[4] Even more important, it was demonstrated experimentally that Mn_3Ge films can be well grown on MgO and Cr-buffered MgO substrates,[6,7,10] which opens numerous opportunities for the MTJs geometry setups and improvements. There is a growing number of publications during the last few years on the TMR effect in the Mn_3Ga and Mn_3Ge films. Here we direct our attention to another possible route of using ferrimagnetic materials with strong spin-orbit induced anisotropy in spintronics devices based on the Tunneling Anisotropic Magneto-resistance (TAMR) effect.

The conventional ferromagnetic based anisotropic magneto-resistance (AMR) spin-valves have been always considered as a possible alternative for developing memory storage devices.[11] The AMR and TAMR effects are directly related to the electronic structure anisotropy induced by spin-orbit coupling (SOC) effects, and the AMR (TAMR) devices can contain only a single magnetic layer. Soft ferromagnet films like Permalloy, where a small AMR effect is present even in the bulk,[12] are usually used in the AMR (TAMR) multilayer systems.[11] The subtle SOC origin of the AMR effect and difficulties for achieving an effective performance at small dimensions required for high-density recording leads to the dominance of technologies based on the Giant Magneto-resistance effects and TMR. Several ideas have reinforced the research in the field of TAMR in the recent decade.[13–17] In particular, the prospective of use of an antiferromagnetic material instead of a ferromagnet as active magnetic layer in TAMR spin-valve was suggested theoretically[18] and then demonstrated experimentally.[19] This suggestion relies on the fact that antiferromagnets can provide more robust anisotropy properties required for sizable TAMR than the best of the conventional ferromagnets.[20,21]

The idea of an antiferromagnetic spintronic device has also been experimentally explored later in connection with the conventional TMR effect.[22] Various ways of utilizing the AFM layer, staggered magnetization direction, have been explored and proposed, including all electrical,[23] exchange springs[19] and strain induced[18] switching. Nevertheless the problem of switching seems to remain the major bottleneck for the application of AFM spintronics. We advocate here that a promising alternative between FM and AFM spintronics based on the TAMR effect might be the use of ferrimagnetic materials, which keeps all advantages of AFM (strong SOC induced electronic anisotropy) and FM materials (magnetization which can be influenced and switched by an external magnetic field). The ferrimagnet switching might be assisted by an external field in addition to the various switching mechanisms explored for AFM (like, e.g., in Ref. 19) sharing the same advantages of AFM intensively studied during recent years (pinning of the domain wall motions, strong PMA, etc.).

Moreover, recent progress achieved in the ultra-fast switching of ferrimagnetic magnetization by short

a)sk@cms.tuwien.ac.at

(femtosecond) laser pulses[24,25] makes the ferrimagnetic based TAMR devices with a single magnetic layer to become a very important emerging field of research. In this letter, we show by comparison of *ab-initio* calculated SOC induced anisotropies of the electronic properties that the ferrimagnetic tetragonal Mn_3Ge alloy exhibits a sizable TAMR, with larger magnitude than the other known Mn based alloys.

Our calculations of the tetragonal DO_{22} τ-phases of Mn_3Ge and Mn_3Ga alloys are done for the experimental lattice constants $a = 3.816$ Å and $b = 7.291$ Å for Mn_3Ge[3] and $a = 3.91$ Å and $b = 7.12$ Å for Mn_3Ga.[26] The $D0_{22}$ τ-phase can be seen as a strongly distorted $L2_1$ full Heusler structure with two non-equivalent Mn sites 2*b* and 4*d*. The opposite orientation of the magnetizations of Mn(2*b*) and Mn(4*d*) sub-lattices are triggered by a strong antiferromagnetic nearest neighbor (NN) coupling, which dominates the rest of the inter-atomic couplings. In Fig. 1 we show the calculated distant inter-atomic exchange interactions, J_{ij}, related to a classical Heisenberg Hamiltonian

$$H = \sum_{i,j\in\{Mn\}} J_{ij}\vec{e}_i\vec{e}_j, \tag{1}$$

where $\vec{e}_i$ are the unit vectors of the spin direction on the *i*-th Mn site and the summation runs over all Mn sites. The exchange interactions were calculated for the reference paramagnetic state of the Mn_3Ge alloy derived within the Disordered Local Moment approximation[27] in combination with the *ab-initio* Local Spin-Density Approximation (LSDA).[28] To this end we use a Green Function based magnetic force theorem[29] embedded[30] in the Korringa-Kohn-Rostokker (KKR) method.[31] Further details of these methods can be found in Ref. 32 where they were applied to calculate the exchange interactions in various structural modifications of Mn_3Ga alloys.[32] Similarly to the case of Mn_3Ga discussed in detail in Ref. 32, the distant interactions beyond the first nearest neighbor (NN) shell within the Mn(4d) sublattice provide a substantial contribution to the high Neel temperature of Mn_3Ge (see Fig. 1). As seen from Fig. 1, the large magnetic ordering temperature of tetragonal Mn_3Ge is partially due to a considerably large third NN coupling within the Mn(4d) sub-lattice, and bears a close similarity to the case of Mn_3Ga.[32] Monte-Carlo simulations for the Hamiltonian Eq. (1) using the calculated exchange constants given in Fig. 1 yield a magnetic ordering temperature around 705 K, in good agreement with the experimental estimate of 800 K.[3] Similar to the case of Mn_3Ga, this value is also underestimated by about 100 K. This indicates[32] that moderate correlation effects, which tend to increase the Mn moments compared to bare LSDA results, may play a role.

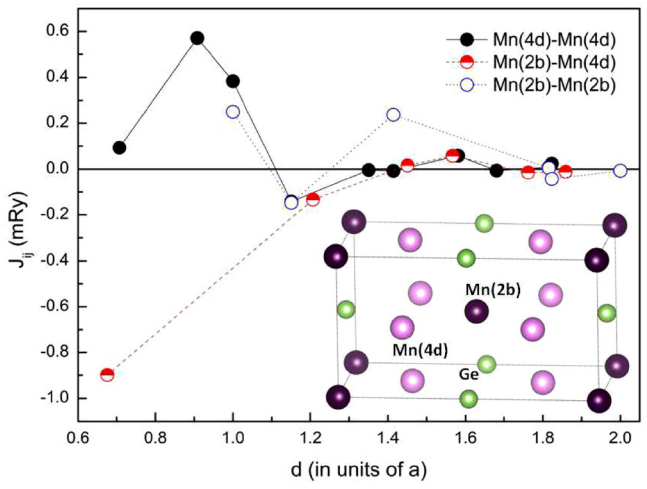

FIG. 1. Calculated exchange interactions in Mn3Ge as a function of the interatomic distance in terms of the in-plane tetragonal lattice constant in the DLM state. Closed symbols: the interactions within the Mn(4d) sublattice, open symbols—Mn(2b), and semi-closed symbols in the intersublattice Mn(2b)-Mn(4d) interactions. Inset: the tetragonal unit cell of Mn3(Ge,Ga). The Mn positions are shown with different shades of magenta.

The exchange interactions calculated in the ferrimagnetic ground state are shown in the supplementary material, Fig. S1. They differ from those calculated in the paramagnetic Disordered Local Moments (DLM) state and ought to be used only for estimation of the low temperature properties. However, their values are irrelevant to the calculation of the Neel transition temperature, as discussed in detail in Ref. 32 for the case of Mn_3Ga.

In the following discussion on the magnetic and electronic structure anisotropy effects, we rest on full potential calculations within the framework of the Full potential Linear Augmented Plane Waves (FLAPW) method[33] with SOC included as described in Ref. 34. In Table I, we show the calculated magnetic moments of the τ-phases of Mn_3Ge and Mn_3Ga in the ferrimagnetic ground state (with moments oriented along the easy *c*-axis). The total M_S per unit cell are in excellent agreement with KKR results for Mn_3Ga (1.71 μ_B) and Mn_3Ge (0.99 μ_B) for the ferrimagnetic ground state. The element specific values for M_S differ slightly (by less than 5%) from the KKR values due to a difference between the unit cell space partition in the FLAPW and the KKR methods. The total magnetization of Mn_3Ge is much lower than that of the Mn_3Ga almost entirely due to differences in the magnetic moments of the Mn(4*d*) sites. Indeed these 4*d*-sites provide the major contribution to the uniaxial magnetic anisotropy (and consequently to the PMA in thin films) in both alloys.

The magneto-crystalline anisotropy energy (MAE) is evaluated using the torque method as described in Ref. 35. For the case of tetragonal symmetry, the phenomenological total energy dependence on the spin quantization direction reads

$$E(\theta,\phi) = K_{2\perp}\sin^2\theta, \tag{2}$$

TABLE I. Spin (M_S) and orbital (M_L) magnetic moments in the MT-sphere of the Mn and Ga/Ge atoms (in Bohr magnetons) and the total M_S per unit cell. In all calculations, the magnetization is directed along the *z*-axis.

Mn_3Ga	Ga[2a]	Mn[2b]	Mn[4d]	Total
M_S	−0.03	−2.85	2.27	1.72
M_L	−0.00	−0.01	0.02	
Mn_3Ge	Ge[2a]	Mn[2b]	Mn[4d]	Total
M_S	−0.04	−2.86	1.95	0.99
M_L	−0.00	−0.02	0.02	

and the corresponding torque is given by, $T(\theta,\phi) = dE(\theta,\phi)/d\theta = \sin 2\theta\,[K_{2\perp}]$. Here $K_{2\perp}$ is the uniaxial MAE constant. The uniaxial magnetic anisotropy energy difference between the in-plane [100] and the out-of-plane [001] magnetization directions, $\mathrm{MAE} = E(\theta = \frac{\pi}{2}, \phi = 0) - E(\theta = 0, \phi = 0)$, is then equal to the value of the torque $T(\theta = \frac{\pi}{4}, \phi = 0)$. The advantage of this approach is that it allows us to split the total uniaxial MAE into element-specific contributions from different atoms in the unit cell. The total MAE and the element specific anisotropy contributions were calculated with accuracy better than 0.01 meV/f.u.

The total and element specific anisotropy constants are shown in Table II. The total uniaxial MAE of Mn_3Ga is somewhat higher than in Mn_3Ge (0.91 against 0.78 meV/f.u.) and both are in good agreements with the earlier FLAPW results derived in Refs. 3 and 9. In the case of Mn_3Ga alloys, we can compare our present MAE results with the Projected Augmented Wave method (VASP code[36]) calculations where the SOC is implemented as described in Ref. 37. In these VASP calculations, the MAE was evaluated directly in terms of the total energy difference for the moments oriented along [100] and [001] crystallographic directions. The MAE value of 0.96 meV/f.u. was obtained with the VASP code, which agrees very well with torque based FLAPW value of 0.91 meV/f.u.

As follows from the element-specific MAE shown in Table II, the Mn(4*d*)-sites provide the major contribution to the uniaxial magnetic anisotropy (and consequently to the PMA in thin films), whereas a small contribution from Mn(2*b*) sites have even different signs in Ge- and Ga-based alloys. Thus the Mn(4*d*) site mainly determines the magnetic anisotropic properties of these materials. Note that the MAE reduction from Mn_3Ga to Mn_3Ge can be directly associated with corresponding reduction of the magnitude of the magnetic moments on the Mn(4*d*) sites in Mn_3Ge from the Mn_3Ga values. These conclusions are qualitatively consistent with previously reported results,[9] where the SOC constant λ was varied for different atomic species in order to determine the element specific MAE contributions.

The large value of the MAE suggests strong SOC effects on the electronic structure of the alloy and is crucially important for the thermal stability in conventional TMR devices providing a large PMA in thin films. Previous studies of the TAMR in ferromagnets and anti-ferromagnets have shown that anisotropic magneto-resistance phenomena can be extended from bulk to nanoscale devices. The TAMR can have large magnitudes, and does not require spin-coherent transport through the structure. For FM and AFM tunneling devices, it has been demonstrated that a useful qualitative analysis of the differential TAMR can be obtained by considering its proportionality to the energy dependent anisotropy in the density of states (ADOS) in the magnetic layer with respect to the crystallographic orientation of the magnetic moments.[18,21] We emphasize that these calculations are only approximate as they neglect the anisotropy of the tunneling matrix elements between wavefunctions in the magnetic and nonmagnetic layers of the TAMR structure.

TABLE II. The element-specific MAE, and the total MAE per unit cell (meV) for Mn_3Ga and Mn_3Ge.

Mn_3Ga	Ga[2a]	Mn[2b]	Mn[4d]	Total
MAE	0.03	0.02	0.86	0.91
Mn_3Ge	Ge[2a]	Mn[2b]	Mn[4d]	Total
MAE	0.05	−0.01	0.74	0.78

The total DOS for Mn_3Ge with the magnetization aligned along the easy [001] axis together with the d-orbital projected DOS for Mn atoms at [2b], and [4d] crystallographic positions is shown in Fig. 2 (upper panel). It is seen that the Mn[4d] gives the main contribution to the DOS spin-polarization near the Fermi energy. In Fig. 2 (lower panel), we show the calculated energy-dependent ADOS of Mn_3Ge and Mn_3Ga. One can see that the ADOS of Mn_3Ge is reaching values up to 10% slightly above the Fermi level. It is much larger than the corresponding values of the Mn_3Ga ADOS and also outnumbers the widely used strongly anisotropic AFM system MnIr.[19] These values are also superior to what can be found in high performance ferromagnets.[20] It

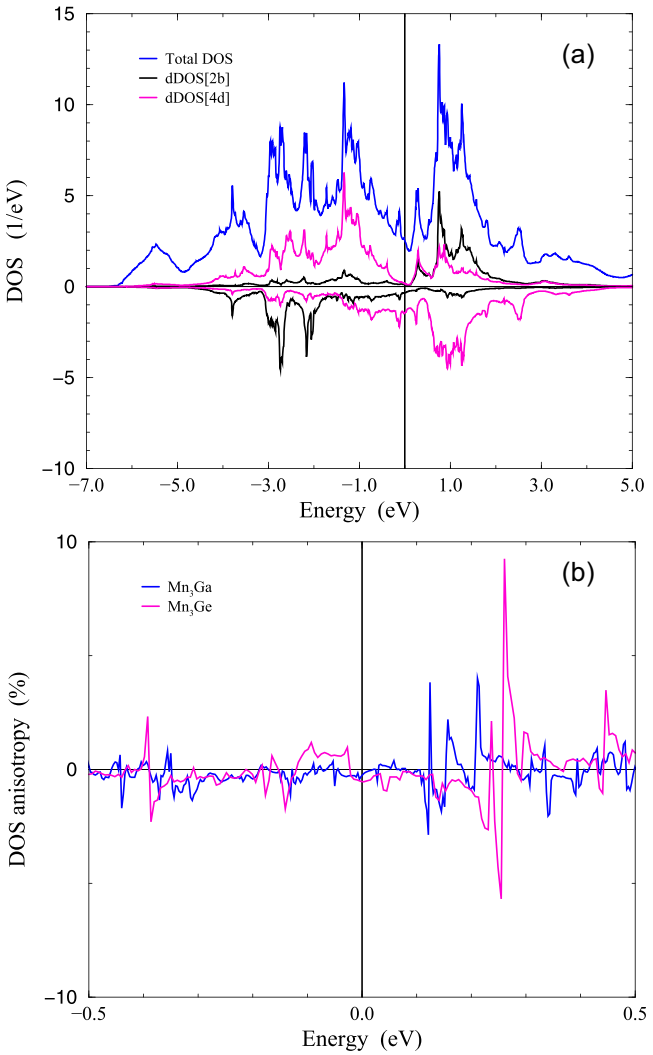

FIG. 2. The total electron density of states (DOS) per formula unit for Mn_3Ge and the magnetization aligned along the easy [001] axis; the d-orbital projected DOS for Mn atoms at [2b], and [4d] crystallographic positions (upper panel). Out-of-plane ADOS = [DOS($\frac{\pi}{2}$, 0)-DOS(0,0)]/DOS(0,0) for the hard [100] and easy [001] axes of Mn_3Ga and Mn_3Ge (lower panel).

thus appears that Mn_3Ge is the most promising candidate for showing a considerable TAMR effect and for a possible application in ferrimagnetic based spintronics, despite that it has a slightly smaller value of the PMA and total magnetization than its Mn_3Ga and AFM counterparts.

In summary, we propose and advocate on the basis of the *ab-initio* band structure calculations, the prospective application of Mn_3Ge alloys for the TAMR based devices. It provides an opportunity for developing all around, the ferrimagnetic memory elements operating with a single active magnetic layer, which might open a route for effective merging of (T)AMR and ultra-fast femtosecond laser switching technology.

See supplementary material for Figure S1 with the exchange interactions calculated in the ferrimagnetic ground state of Mn_3Ge.

The authors acknowledge the financial support of the Austrian Science Foundation (FWF) ViCoM Project No. F4109-N28 (S.K. and P.M.), and the Czech Republic GACR Grant No. 14-37427G (A.B.S.).

[1]*Handbook of Spin Transport and Magnetism*, edited by E. Y. Tsymbal and I. Zutic (CRC Press, London/New York, 2012).
[2]H. Kurt and J. M. D. Coey, in *Heusler Alloys: Properties, Growth, Applications*, edited by C. Felsner and A. Hirohata (Springer, Cham/Heidelberg/London/New York, 2016), pp. 167–192.
[3]H. Kurt, N. Baadji, K. Rode, M. Venkatesan, P. Stamenov, S. Sanvito, and J. M. D. Coey, Appl. Phys. Lett. **101**, 132410 (2012).
[4]A. Sugihara, K. Suzuki, T. Miyazaki, and S. Mizukami, Jpn. J. Appl. Phys., Part 1 **54**, 078002 (2015).
[5]J. Jeong, Y. Ferrante, S. V. Faleev, M. G. Samant, C. Felser, and S. S. P. Parkin, Nat. Commun. **7**, 10276 (2016).
[6]S. Mizukami, A. Sakuma, A. Sugihara, T. Kubota, Y. Kondo, H. Tsuchira, and T. Miyazaki, Appl. Phys. Express **6**, 123002 (2013).
[7]A. Sugihara, K. Suzuki, S. Mizukami, and T. Miyazaki, J. Phys. D: Appl. Phys. **48**, 164009 (2015).
[8]B. Balke, G. H. Fecher, J. Winterlik, and C. Felser, Appl. Phys. Lett. **90**, 152504 (2007).
[9]K. Rode, N. Baadji, D. Betto, Y.-C. Lau, H. Kurt, M. Venkatesan, P. Stamenov, S. Sanvito, J. M. D. Coey, E. Fonda, E. Otero, F. Choueikani, P. Ohresser, F. Porcher, and G. André, Phys. Rev. B **87**, 184429 (2013).
[10]A. Sugihara, S. Mizukami, Y. Yamada, K. Koike, and T. Miyazaki, Appl. Phys. Lett. **104**, 132404 (2014).
[11]C.-J. Zhao, L. Ding, J.-S. Huang Fu, J.-Y. Zhang, and G.-H. Yu, Rare Met. **32**, 213 (2013).
[12]S. Khmelevskyi, K. Palotas, L. Szunyough, and P. Weinberger, Phys. Rev. B **68**, 012402 (2003).
[13]C. Gould, C. Rüster, T. Jungwirth, E. Girgis, G. M. Schott, R. Giraud, K. Brunner, G. Schmidt, and L. W. Molenkamp, Phys. Rev. Lett. **93**, 117203 (2004).
[14]J. Velev, R. F. Sabirianov, S. S. Jaswal, and E. Y. Tsymbal, Phys. Rev. Lett. **94**, 127203 (2005).
[15]J. Wunderlich, T. Jungwirth, B. Kaestner, A. C. Irvine, A. B. Shick, N. Stone, K.-Y. Wang, U. Rana, A. D. Giddings, C. T. Foxon, R. P. Campion, D. A. Williams, and B. L. Gallagher, Phys. Rev. Lett. **97**, 077201 (2006).
[16]B. G. Park, J. Wunderlich, D. A. Williams, S. J. Joo, K. Y. Jung, K. H. Shin, K. Olejnik, A. B. Shick, and T. Jungwirth, Phys. Rev. Lett. **100**, 087204 (2008).
[17]R. W. Li, H. B. Wang, X. W. Wang, X. Z. Yu, Y. Matsui, Z.-H. Cheng, B.-G. Shen, E. W. Plummer, and J. D. Zhang, Proc. Natl. Acad. Sci. U.S.A. **106**, 14224 (2009).
[18]A. B. Shick, S. Khmelevskyi, O. N. Mryasov, J. Wunderlich, and T. Jungwirth, Phys. Rev. B **81**, 212409 (2010).
[19]B. G. Park, J. Wunderlich, X. Marti, V. Holy, Y. Kurosaki, M. Yamada, H. Yamamoto, A. Nishide, J. Hayakawa, H. Takahashi, A. B. Shick, and T. Jungwirth, Nat. Mater. **10**, 347 (2011).
[20]A. B. Shick, F. Máca, J. Mašek, and T. Jungwirth, Phys. Rev B **73**, 024418 (2006).
[21]A. B. Shick, F. Máca, M. Ondráček, O. N. Mryasov, and T. Jungwirth, Phys. Rev. B **78**, 054413 (2008).
[22]L. Wang, S. G. Wang, S. Rizwan, Q. H. Qin, and X. F. Han, Appl. Phys. Lett. **95**, 152512 (2009).
[23]E. Plekhanov, A. Stroppa, and S. Picozzi, J. Appl. Phys. **120**, 074104 (2016).
[24]A. Kirilyuk, A. V. Kimel, and Th. Rasing, Rev. Mod. Phys. **82**, 2731 (2010).
[25]R. F. L. Evans, T. A. Ostler, R. W. Chantrell, I. Radu, and T. Rasing, Appl. Phys. Lett. **104**, 082410 (2014).
[26]H. Kurt, K. Rode, M. Venkatesan, P. Stamenov, and J. M. D. Coey, Phys. Status Solidi B **248**, 2338 (2011).
[27]B. L. Gyorffy, A. J. Pindor, J. Staunton, G. M. Stocks, and H. Winter, J. Phys. F: Met. Phys. **15**, 1337 (1985).
[28]U. von Barth and L. Hedin, J. Phys. C **5**, 1629–1642 (1972).
[29]A. I. Lichtenstein, M. I. Katsnelson, V. P. Antropov, and V. A. Gubanov, J. Magn. Magn. Mater. **67**, 65 (1987).
[30]A. V. Ruban, S. I. Simak, S. Shallcross, and H. L. Skriver, Phys. Rev. B **67**, 214302 (2003).
[31]A. V. Ruban and H. L. Skriver, Comput. Mater. Sci. **15**, 119 (1999).
[32]S. Khmelevskyi, A. V. Ruban, and P. Mohn, Phys. Rev. B **93**, 184404 (2016).
[33]D. J. Singh, *Planewaves, Pseudopotentials and the LAPW Method* (Kluwer Academic, Boston, 1994), p. 115.
[34]A. B. Shick, D. L. Novikov, and A. J. Freeman, Phys. Rev. B **56**, R14259 (1997).
[35]S. Khmelevskyi, A. B. Shick, and P. Mohn, Phys. Rev. B **83**, 224419 (2011).
[36]G. Kresse and J. Furthmüller, Phys. Rev. B **54**, 11169 (1996).
[37]S. Steiner, S. Khmelevskyi, M. Marsmann, and G. Kresse, Phys. Rev. B **93**, 224425 (2016).